Int. J. Multiphase Flow Vol. 7, pp. 245–260, 1981
Printed in Great Britain

0301-9322/81/030245-16$02.00/0
Pergamon/Elsevier

THE SLOW ROTATION OF AN AXISYMMETRIC SOLID SUBMERGED IN A FLUID WITH A SURFACTANT SURFACE LAYER—II

THE ROTATING SOLID IN A BOUNDED FLUID

R. SHAIL and D. K. GOODEN

Department of Mathematics, University of Surrey, Guildford, Surrey GU2 5XH, England

(*Received* 4 *June* 1980; *in revised form* 2 *June* 1980)

Abstract—This paper extends the work in Shail (1979) on the problem of an axisymmetric submerged solid rotating slowly and steadily in a fluid whose surface is covered with a surfactant film. The bulk fluid is of finite extent, and both asymptotic and numerical results (the latter in the case of a thin circular disk) are given for boundary effects on the resistive torque and surface velocity profile when the container is a right circular cylinder and the fluid is of finite depth.

1. INTRODUCTION

In the first paper of this series (Shail 1979), hereafter referred to as I, the problem of an axisymmetric solid rotating in the presence of a fluid surface covered with a monomolecular surfactant film was considered. The bulk substrate fluid in I is taken to be *semi-infinite* in extent, and the fluid motion generated by the rotating solid is axisymmetric, steady and sufficiently slow to permit linearisation of the equation of motion satisfied by the azimuthal component of fluid velocity. The aim of the work, in which the rotating solid is a thin circular disk, is the investigation of viscometric methods for the measurement of η, the coefficient of surface shear viscosity of adsorbed film; the alternative case of a rotating sphere has been treated by Davis & O'Neill (1979).

The presence of the surfactant film influences the friction couple on the solid, and the analysis in I provides sufficient information to allow an evaluation of η. However, the proximity of finite boundaries of the fluid container also influences the couple, and an accurate determination of η therefore requires a consideration of container boundary effects.

It is the purpose of this paper to supply a suitable analysis of boundary effects, again with particular emphasis on the rotating disk viscometer of I. The integral equation approach developed in I is summarised in the next section, and the appropriate Green's function for a right cylindrical container is given. In section 3 asymptotic results for the friction couple, valid for an arbitrary axisymmetric rotator, are developed for the case when the rotating body is far from the fluid boundaries, thus generalising to surfactant situations the results of Brenner (1961) and others.

In section 4 the techniques of I are used to reduce the rotating-disk problem to the solution of a Fredholm integral equation of the second kind, and a description is given of the numerical treatment of this equation. Section 5 contains a representative sample of the extensive numerical results which have been obtained for both the frictional couple on the rotating disk, and the surface fluid velocity profile. The Appendix to the paper contains a derivation of the Green's function used, a calculation which requires the expansion of a function in terms of a complete, but *non-orthogonal*, set.

2. BASIC EQUATIONS

A vertical right circular cylindrical container of radius b and height H is filled with incompressible viscous fluid whose plane horizontal surface is covered with an adsorbed monomolecular film. A totally immersed solid with surface S rotates slowly in the fluid about a vertical axis of symmetry, common to the container and the solid, with constant angular speed

Ω. A suitably chosen centre 0 of the solid is at a distance $h(<H)$ below the surface of the fluid.

Referring to the geometrical description and cyclindrical polar coordinates (ρ, ϕ, z) at 0 introduced in section 2 of I, the wetted surface S_1 of the fluid container is defined by

$$\rho = b, -h \leq z \leq H-h,$$

$$z = H-h, 0 \leq \rho \leq b,$$

and the surface film S_2 occupies the region

$$z = -h, 0 \leq \rho \leq b,$$

all with $0 \leq \phi < 2\pi$. The azimuthal component $v(\rho, z)$ of fluid velocity satisfies the linearized Navier–Stokes equation

$$\frac{\partial^2 v}{\partial \rho^2} + \frac{1}{\rho}\frac{\partial v}{\partial \rho} + \frac{\partial^2 v}{\partial z^2} - \frac{v}{\rho^2} = 0, \qquad [1]$$

the no-slip conditions

$$v(\rho, z) = \Omega\rho, (\rho, z) \in S, \qquad [2]$$

$$v(\rho, z) = 0, (\rho, z) \in S_1, \qquad [3]$$

and

$$\frac{\partial v}{\partial z} - \lambda\frac{\partial^2 v}{\partial z^2} = 0 \text{ on } z = -h, 0 \leq \rho \leq b, \qquad [4]$$

where $\lambda = \eta/\mu$ is the ratio of the surface shear viscosity η to the bulk fluid viscosity μ.

As shown in I, the problem of finding v is reducible to that of determining a source density $\sigma(\rho, z)$, $(\rho, z) \in S$, which satisfies the integral equation

$$\Omega\rho = \pi\int_C \sigma(\rho', z')G^{(1)}(\rho, z; \rho', z')\rho' \mathrm{d}l, (\rho', z') \in C, \qquad [5]$$

where C is the bounding curve of S in a meridional plane and $\mathrm{d}l'$ denotes the element of arc length of C. In [5]

$$\sigma(\rho, z) = -\frac{1}{4\pi}\rho\frac{\partial}{\partial n}\left(\frac{v}{\rho}\right),$$

and $G^{(1)}(\rho, z; \rho', z')$ is the coefficient of $\cos(\phi - \phi')$ in the Fourier expansion of the Green's function $G(\rho, z, \phi; \rho', z', \phi')$ which satisfies the equation

$$\nabla^2 G = -\frac{4\pi}{\rho}\delta(\rho-\rho')\delta(\phi-\phi')\delta(z-z'), \qquad [6]$$

and conditions [3] and [4]. The problem of determining G is treated in the Appendix, where it is shown that

$$G^{(1)}(\rho, z; \rho', z') = 2\int_0^\infty J_1(\xi\rho)J_1(\xi\rho')e^{-\xi|z-z'|}d\xi + 2\int_0^\infty [(1-\lambda\xi)\{e^{-\xi(2h-H)}\cosh(\xi(z+z'))$$

$$-e^{-\xi H}\cosh(\xi(z-z'))\} - e^{-\xi(z+z')}\{\cosh(\xi(2h-H)$$

$$+\lambda\xi\sinh(\xi(2h-H))\}]\frac{J_1(\xi\rho)J_1(\xi\rho')}{\cosh\xi H + \lambda\xi\sinh\xi H}d\xi$$

$$-16\sum_{n=1}^{\infty}\frac{p_n K_1(p_n b)}{(2Hp_n + \sin 2Hp_n)I_1(p_n b)}I_1(p_n\rho)I_1(p_n\rho')\sin\{p_n(z-H+h)\}\sin\{p_n(z'-H+h)\}, \quad [7]$$

where p_n, $n = 1, 2, 3\ldots$, are the positive roots of the equation

$$\cos p_n H - \lambda p_n \sin p_n H = 0. \quad [8]$$

In terms of σ the frictional couple N acting on the solid is

$$N = -8\pi^2\mu\int_C \rho^2\sigma(\rho, z)dl. \quad [9]$$

3. ASYMPTOTIC RESULTS

In this section we discuss the asymptotic solution of [5] in the case when a/h, a/H and a/b are small compared with unity, a being a typical dimension of the rotating body. Whilst this situation is not of such great practical importance, the methods used and formulae obtained are of some theoretical interest, providing an extension and alternative derivation of the results of Brenner (1961) on boundary effects. In the following analysis it is assumed that the small quantities a/h, a/H and a/b are all of the same order; thus $O(a/h)$ is to be interpreted as $O(a/h, a/H, a/b)$. We write

$$G^{(1)} = G_0^{(1)} + G_1^{(1)}, \quad [10]$$

where

$$G_0^{(1)} = 2\int_0^\infty J_1(\xi\rho)J_1(\xi\rho')e^{-\xi|z-z'|}d\xi. \quad [11]$$

In [10] $G_0^{(1)}$ is the coefficient of $\cos(\phi'-\phi)$ in the expansion of the singular inverse distance Green's function in cylindrical coordinates, and $G_1^{(1)}$ is regular at $\rho = \rho'$, $z = z'$. By direct expansion of [7] it may be verified that

$$G_1^{(1)} = \frac{1}{h^3}A\rho\rho' + \frac{1}{h^4}B\rho\rho'(z+z') + O\left(\frac{a^5}{h^5}\right) \quad [12]$$

as $h\to\infty$, where A and B (which depend on the ratio λ/h) are constants with

$$A = \lim_{\rho,\rho'\to 0} h^3 G_1^{(1)}(\rho, 0; \rho', 0)/\rho\rho'. \quad [13]$$

We now develop $\sigma(\rho, z)$ as

$$\sigma(\rho, z) = \sigma_0(\rho, z) + \frac{1}{h^3}\sigma_1(\rho, z) + \frac{1}{h^4}\sigma_2(\rho, z) + \ldots, \quad [14]$$

where $h^{-1}\sigma_{i+1}(\rho, z) = O(\sigma_i(\rho, z))$ as $h \to \infty$, and σ_0 is the source density appropriate to a solid rotating in an infinite fluid. Substituting [12] and [14] into [5] we determine the σ_i by the sequence of integral equations

$$\pi \int_C \sigma_0(\rho', z')G_0^{(1)}(\rho, z; \rho' z')\rho' \mathrm{d}l' = \Omega\rho, \tag{15}$$

$$\int_C \sigma_1(\rho', z')G_0^{(1)}(\rho, z; \rho', z')\rho' \mathrm{d}l' = -A\rho \int_C \rho'^2\sigma_0(\rho', z')\mathrm{d}l', \tag{16}$$

$$\int_C \sigma_2(\rho', z')G_0^{(1)}(\rho, z; \rho', z')\rho' \mathrm{d}l' = -B\rho \int_C \rho'^2(z+z')\sigma_0(\rho', z')\mathrm{d}l', \tag{17}$$

where $(\rho, z) \in C$. Comparing [15] and [16] it follows that

$$\sigma_1(\rho, z) = -\frac{\pi}{\Omega} A\left\{\int_C \rho'^2\sigma_0(\rho', z')\mathrm{d}l'\right\}\sigma_0(\rho, z). \tag{18}$$

Further, from [9]

$$\begin{aligned} N &= -8\pi^2\mu\left\{\int_C \rho^2\sigma_0(\rho, z)\mathrm{d}l + \frac{1}{h^3}\int_C \rho^2\sigma_1(\rho, z)\mathrm{d}l + \frac{1}{h^4}\int_C \rho^2\sigma_2(\rho, z)\mathrm{d}l + O\left(\frac{a_5}{h^5}\right)\right. \\ &= N_\infty - \frac{A}{8\pi\mu\Omega h^3}N_\infty{}^2 - \frac{8\pi^2\mu}{h^4}\int_C \rho^2\sigma_2(\rho, z)\mathrm{d}l + O\left(\frac{a^5}{h^5}\right), \end{aligned} \tag{19}$$

where N_∞ is the couple on the solid in an unbounded medium.

To evaluate the final integral in [19] we multiply [17] by $\rho\sigma_0(\rho, z)$ and integrate along C, whence

$$\begin{aligned} &\int_C \sigma_0(\rho, z)\left\{\int_C \sigma_2(\rho, z)G_0^{(1)}(\rho, z; \rho', z')\rho' \mathrm{d}l'\right\}\rho \mathrm{d}l \\ &= -B\int_C\int_C \rho^2\rho'^2(z+z')\sigma_0(\rho, z)\sigma_0(\rho', z')\mathrm{d}l\mathrm{d}l'. \end{aligned}$$

Inverting orders of integration and using [15], it follows that

$$\frac{\Omega}{\pi}\int_C \rho^2\sigma_2(\rho, z)\mathrm{d}l = -2B\int_C \rho^2 z\sigma_0(\rho, z)\mathrm{d}l \int_C \rho'^2\sigma_0(\rho', z')\mathrm{d}l', \tag{20}$$

and by a suitable choice of the origin 0 we can ensure that the penultimate integral in [20] vanishes. Thus [19] can be written as

$$\frac{N}{N_\infty} = 1 - A\frac{N_\infty}{8\pi\mu\Omega h^3} + O\left(\frac{a^5}{h^5}\right). \tag{21}$$

For the container under consideration [7] and [13] show that

$$A = h^3(\alpha - 4\beta), \tag{22}$$

where

$$\alpha = \frac{1}{2}\int_0^\infty \frac{\xi^2[(1-\lambda\xi)\{e^{-\xi(2h-H)} - e^{-\xi H}\} - \{\cosh \xi(2h-H) + \lambda\xi \sinh \xi(2h-H)\}]}{\cosh \xi H + \lambda\xi \sinh \xi H}\mathrm{d}\xi \tag{23}$$

and

$$\beta = \sum_{n=1}^{\infty} \frac{p_n^3 K_1(p_n b)\sin^2 p_n(H-h)}{(2Hp_n + \sin 2p_n H)I_1(p_n b)} \tag{24}$$

and we can delineate a number of cases of which the following seem to be of most interest.

Firstly, suppose that $\Lambda = \lambda/h = O(1)$, i.e. $\eta/\mu a \gg 1$ since $a/h \ll 1$, corresponding to a very viscous surface film. Then putting $t = \xi h$ in [23] and $\sigma_n = Hp_n$ in [24], [21] and some manipulation show that

$$\frac{N}{N_\infty} = 1 - \frac{N_\infty}{8\pi\mu\Omega h^3}\left[\frac{1}{2}\int_0^\infty \frac{t^2[(1-\Lambda t)e^{-2t} - e^{-2pt}\{2(1-\Lambda t) + e^{2t}(1+\Lambda t)\}]}{(1+e^{-2pt})(1+\Lambda t\tanh pt)}\,dt \right.$$
$$\left. - \frac{4}{p^3}\sum_{n=1}^{\infty}\frac{\sigma_n^3 K_1(\sigma_n q)\sin^2\{\sigma_n(1-p^{-1})\}}{(2\sigma_n + \sin 2\sigma_n)I_1(\sigma_n q)}\right] + O\left(\frac{a^5}{h^5}\right), \tag{25}$$

where $p = H/h$†, $q = b/H$, both of order unity, and $n\pi < \sigma_n < (n+1/2)\pi$.

Secondly, suppose that $a/h \ll 1$, with $\eta/\mu a = O(1)$ and $\Lambda = O(a/h)$. Then the result [25] can be simplified by evaluating the integral and infinite series asymptotically for small Λ. An elementary application of Watson's lemma and subsequent integration show that the infinite integral in [25] has the asymptotic development

$$-\frac{3}{8p^3}\zeta(3) + \frac{1}{4}\sum_{j=-\infty}^{\infty}\frac{(-1)^j}{|jp-1|^3} - 2\Lambda\int_0^\infty t^3\left\{\frac{\sinh(p-1)t}{\cosh pt}\right\}^2 dt + O(\Lambda^2) \tag{26}$$

as $\Lambda \to 0$.

To estimate the infinite series asymptotically we first note the identity

$$\sum_{n=}^{\infty}\frac{\sigma_n^3 K_1(\sigma_n q)\sin^2\sigma_n s}{(2\sigma_n + \sin 2\sigma_n)I_1(\sigma_n q)} = \frac{1}{2}\sum_{n=1}^{\infty}\frac{n^2\pi^2 K_1(n\pi q)\sin^2 sn\pi}{I_1(n\pi q)}$$
$$-\frac{1}{4\pi i}\int_\Gamma \frac{z^2 K_1(qz)\sin^2 sz}{\sin z(\cos z - p^{-1}\Lambda z\sin z)}\,dz, \tag{27}$$

where $s = 1 - p^{-1}$ and the contour Γ is the imaginary axis in the z-plane, indented into the right-hand half-plane at $z = \pm ij_n/q$, where the j_n, $n = 1, 2, \ldots$, are the positive zeros in ascending order of magnitude of $J_1(x)$. The contour integral in [27] can now be expanded asymptotically for small Λ by Watson's lemma, and evaluating the resulting integrals as residue series we find that

$$\sum_{n=1}^{\infty}\frac{\sigma_n^3 K_1(\sigma_n q)\sin^2\sigma_n s}{(2\sigma_n + \sin 2\sigma_n)I_1(\sigma_n q)} = \frac{1}{2}T_1(q, s) - \frac{1}{2}\frac{\Lambda}{p}\{3T_1(q, s)$$
$$+ sT_2(q, s) + T_3(q, s)\} + O(\Lambda^2), \tag{28}$$

where $T_j(q, s)$, $j = 1, 2, 3$, are defined by the following rapidly convergent series:

$$T_1(q, s) = \sum_{n=0}^{\infty}\frac{\epsilon_n^2 K_1(\epsilon_n q)\sin^2\epsilon_n s}{I_1(\epsilon_n q)} \tag{29}$$

†From the geometry of the system $p > 1$, thus ensuring the convergence of the integral in [25]. The numerical computation of the integral and series in [25] present no particular difficulties.

$$T_2(q, s) = \sum_{n=0}^{\infty} \frac{\epsilon_n^3 K_1(\epsilon_n q) \sin 2\epsilon_n s}{I_1(\epsilon_n q)} = \frac{\partial T_1}{\partial s}, \qquad [30]$$

$$T_3(q, s) = -\sum_{n=0}^{\infty} \frac{\epsilon_n^2 \sin^2 \epsilon_n s}{\{I_1(\epsilon_n q)\}^2} = \frac{\partial T_1}{\partial q}, \qquad [31]$$

where $\epsilon_n = (n + 1/2)\pi$.

Collecting together the various results, [25], [26] and [28] show that

$$\frac{N}{N_\infty} = 1 - \frac{N_\infty}{8\pi\mu\Omega}\left[\frac{1}{2h^3}\left\{-\frac{3}{8p^3}\zeta(3) + \frac{1}{4}\sum_{j=-\infty}^{\infty}\frac{(-1)^j}{|jp-1|^3}\right.\right.$$
$$\left. - \frac{2\lambda}{h}\int_0^\infty t^3\left(\frac{\sinh(p-1)t}{\cosh pt}\right)^2 dt\right\} - \frac{2}{H^3}\{T_1(q, s)$$
$$\left. - \frac{\lambda}{H}(3T_1(q, s) + sT_2(q, s) + T_3(q, s))\}\right] + O\left(\frac{a^5}{h^5}\right). \qquad [32]$$

Examination of the various series and the integral in [32] show that they are easily computed numerically for specific values of p, q, s, there being exponential damping in all but the first series, which itself presents no problems. In the special case of a sphere ($N_\infty = 8\pi\mu\Omega a^3$) rotating in a stratum of fluid of infinite width ($b \to \infty$), the T_j-series in [32] vanish, and the resulting torque ratio N/N_∞ agrees with that found by Davis & O'Neill (1979).

4. THE ROTATING-DISK PROBLEM

For the remainder of this paper the particular case of the rotation of a thin disk in the bounded fluid is treated. Units are chosen so that the radius of the disk is unity, it being specified by $z = 0, 0 \le \rho \le 1, 0 \le \phi < 2\pi$. As pointed out in I, [5] must be modified to read

$$\Omega\rho = \pi\int_0^1 \sigma^*(\rho', 0)G^{(1)}(\rho, 0; \rho', 0)\rho' d\rho', \qquad [33]$$

where

$$\sigma^*(\rho, 0) = -\frac{\rho}{2\pi}\frac{\partial}{\partial z}\left(\frac{v(\rho, 0)}{\rho}\right). \qquad [34]$$

The couple N is given by

$$N = -8\pi^2\mu\int_0^1 \rho^2\sigma^*(\rho, 0)d\rho. \qquad [35]$$

Proceeding as in I, we replace the integral equation [33] by an equation of the second kind. Defining $\theta(x)$ by

$$\theta(x) = \frac{\Omega x}{2\pi}\int_x^1 \frac{\sigma^*(w, 0)}{(w^2 - x^2)^{1/2}} dw, \qquad [36]$$

then θ is found to satisfy the equation

$$\theta(x) + \int_0^1 L(x, y)\theta(y)dy = 2x, \quad 0 \le x \le 1, \qquad [37]$$

where

$$L(x, y) = -\frac{2}{\pi}\int_0^\infty \frac{2(1-\lambda\xi)e^{-2\xi H} + (1+\lambda\xi)e^{-2(H-h)\xi} - (1-\lambda\xi)e^{-2h\xi}}{(1+\lambda\xi)+(1-\lambda\xi)e^{-2Hj}}$$

$$\times \sin\xi x \sin\xi y \,\mathrm{d}y - \frac{16}{\pi}\sum_{n=1}^{\infty} \frac{p_n K_1(p_n b)\sinh p_n x \sinh p_n y \sin^2 p_n(H-h)}{(2Hp_n + \sin 2p_n H) I_1(p_n b)}. \quad [38]$$

Further, in terms of θ,

$$N = -16\,\Omega \int_0^1 x\theta(x)\mathrm{d}x. \quad [39]$$

It is not possible to solve [37] in closed form for arbitrary λ, h, b and H, and hence numerical methods must be used. Equation [37] has been solved numerically using a NAG library routine based on El Gendi's (1969) method, which first replaces the unknown $\theta(x)$ on $0 \le x \le 1$ by a Chebyshev series of n terms of the form

$$\theta(x) \simeq \sum_{i=1}^{n} c_i T_{i-1}(2x-1). \quad [40]$$

The coefficients c_i, $i = 1, \ldots n$ in [40] are determined from approximate values θ_i, $i = 1, \ldots n$ of the function $\theta(x)$ at a set of n Chebyshev abscissae

$$x_i = \frac{1}{2}[1 + \cos\{(i-1)\pi/(n-1)\}],\ i = 1, \ldots n. \quad [41]$$

Further, the values of θ_i are obtained by solving a set of n simultaneous linear equations, found by applying a quadrature formula, equivalent to that of Clenshaw & Curtis (1960), to [37] at each of the points [41]. Having computed the coefficients c_i, [40] is used to calculate the values of $\theta(x)$ at 21 equally spaced points in the interval $0 \le x \le 1$, and the torque is found from [39] by numerical quadrature.

The procedure employed was to start from $n = 8$ and calculate the solution $\theta(x)$ in the form [40] and the torque for given λ, h, b and H; n was then increased in steps of 2 or 3 until successive values of the torque showed no change correct to 4 decimal places. It was found that as h diminished the value of n required for convergence increased. For example, for $h = 0.25$ the procedure converged when $n = 10$, irrespective of the values of λ, b, H, whereas for $h = 0.125$ the required value of n was 15.

In the formulation of the simultaneous equations described above it is necessary to calculate the values $L(x_i, y_j)$ of the kernel [38] at the Chebyshev points (x_i, y_j). The integration in [38] was performed using a Patterson-type quadrature routine, and as in I it proved necessary to use several forms of the integral to achieve satisfactory convergence. The integral in [38], $L_1(x, y)$ say, can be written as

$$L_1(x, y) = \frac{1}{\pi}\{M(x+y) - M(|x-y|)\}, \quad [42]$$

where

$$M(v) = \int_0^\infty \frac{2(1-\lambda\xi)e^{-\xi H} + (1+\lambda\xi)e^{-2(H-b)\xi} - (1-\lambda\xi)e^{-2h\xi}}{(1+\lambda\xi)+(1-\lambda\xi)e^{-2H\xi}} \cdot \cos v\xi \,\mathrm{d}\xi, \quad [43]$$

and v satisfies the inequality $0 \le v \le 2$. Writing $v\xi = t$, the integral over t is easily evaluated numerically with a suitable finite upper limit, unless for example $v/2h$ is small. To cover this situation a contour integral transformation in which the contour of integration becomes the half-line of unit slope issuing from the origin in the $(t + i\tau)$-plane was used. The resulting integrals then have improved convergence properties, but their length precludes us from quoting them. here.

The summation in the infinite series in [38] at the Chebyshev points (x_i, x_j) was terminated when the modulus of the next term to be added became less than 10^{-11}. The roots p_n of the transcendental equation

$$\cos p_n H - \lambda p_n \sin p_n H = 0$$

were computed using a library iterative routine, use being made of the inequality $n\pi/H < p_n < (n + 1/2)\pi/H$ to establish initial estimates for subsequent rapid convergence.

As indicated in I, a knowledge of the surface velocity profile can be of practical use. To determine $v(\rho, -h)$ the same steps are followed as in I, leading to the form

$$v(\rho, -h) = \frac{4\Omega}{\pi} \int_0^1 \theta(x) \left\{ \int_0^\infty \frac{e^{-h\xi} - e^{-(2H-h)\xi}}{(1+\lambda\xi) + (1-\lambda\xi)e^{-2H\xi}} J_1(\xi\rho) \sin \xi x \, d\xi \right.$$
$$\left. - 4 \sum_{n=1}^{\infty} \frac{p_n I_1(p_n p) K_1(p_n b) \sinh p_n x \sin p_n H \sin p_n (H-h)}{(2Hp_n + \sin 2p_n H) I_1(p_n b)} \right\} dx. \qquad [44]$$

The inner infinite integral in [44] contains oscillatory terms and is also slowly convergent for $h \ll 1$. It does not seem to be possible to transform it as in I to a more rapidly convergent form, but for the computations presented in the results, a Patterson-type integration routine was successfully used to compute for given x and ρ the form

$$\int_0^\infty \frac{e^{-\xi} - e^{-(2p-1)\xi}}{(h+\lambda\xi) + (h-\lambda\xi)e^{-2p\xi}} J_1(\xi\rho/h) \sin(\xi x/h) d\xi,$$

where $p = H/h$, the infinite range of integration being truncated at $\xi = 20$. The summation in [44] was terminated when the modulus of the summand was less than 10^{-6}, and the final evaluation of $v(\rho, -h)$ completed using a library quadrature routine for a discrete function.

5. NUMERICAL RESULTS

In this section the results of our detailed computations of frictional couples and surface velocity profiles are presented. For a rotating disk of unit radius the problem contains four variable parameters, namely λ, h, H and b. Tables 1 and 2 give, for varying λ, values of $N(\lambda)/\mu\Omega$ for $h = 0.125$ and $h = 0.25$ respectively, and for the values (1, 2), (2, 2), (10, 10), (2, 100) and (100, 100) of the ordered pair (H, b). They illustrate clearly the effects of the finite dimensions of the container. The values in the final columns of each table are indistinguishable from the semi-infinite fluid results in I. Further, even when H and b are changed from $H = 100$, $b = 100$ to $H = 10$ and $b = 10$, the percentage change in $N(\lambda)/\mu\Omega$ is everywhere less than 1 percent. However for $H = 1$ and $b = 2$ percentage increases of the order of 10 per cent are found for λ in the range (0, 1), and further reductions in H and b result in even larger percentage increases. It follows that the container boundaries must be sufficiently far from the rotating disk in order to avoid boundary effects masking surfactant effects.

As in I, these tables may be used in conjunction with the method of least squares to give a polynomial representation of λ as a function of N. The results for $0 \le \lambda \le 1$ are illustrated graphically in figures 1 and 2.

A convenient way to exhibit the effect of the surfactant film is afforded by evaluating

Table 1. Values of $N(\lambda)/\mu\Omega$ for $h = 0.125$ and various values of λ, H and b

λ	H = 1.0 b = 2.0	H = 2.0 b = 2.0	H = 10.0 b = 10.0	H = 2.0 b = 100.0	H = 100.0 b = 100.0
0	7.9368	7.6549	7.1810	7.2789	7.1776
0.025	8.2184	7.9357	7.4296	7.5313	7.4260
0.05	8.4811	8.1983	7.6617	7.7668	7.6579
0.075	8.7287	8.4463	7.8807	7.9888	7.8767
0.1	8.9639	8.6822	8.0888	8.1996	8.0846
0.25	10.1833	9.9092	9.1725	9.2950	9.1671
0.5	11.7409	11.4813	10.5767	10.7082	10.5695
0.75	12.9262	12.6793	11.6704	11.8041	11.6617
1.0	13.8646	13.6281	12.5576	12.6900	12.5476
1.25	14.6277	14.3997	13.2960	13.4252	13.2849
1.5	15.2610	15.0401	13.9222	14.0472	13.9102
1.75	15.7953	15.5804	14.4609	14.5812	14.4481
2.0	16.2522	16.0424	14.9298	15.0454	14.9164
3.0	17.5676	17.3721	16.3279	16.4251	16.3126
4.0	18.4015	18.2150	17.2562	17.3385	17.2401
5.0	18.9776	18.7972	17.9193	17.9899	17.9029
6.0	19.3995	19.2234	18.4172	18.4786	18.4009
8.0	19.9760	19.8058	19.1159	19.1642	19.1001
10.0	20.3515	20.1851	19.5831	19.6228	19.5682
50.0	21.7338	21.5810	21.3966	21.4094	21.3907
100.0	21.9292	21.7783	21.6661	21.6772	21.6628
∞	22.1304	21.9814	21.9474	21.9581	21.9474

Table 2. Values of $N(\lambda)/\mu\Omega$ for $h = 0.25$ and various values of λ, H and b

λ	H = 1.0 b = 2.0	H = 2.0 b = 2.0	H = 10.0 b = 10.0	H = 2.0 b = 100.0	H = 100.0 b = 100.0
0	9.3223	8.8626	8.2457	8.3797	8.2413
0.025	9.5102	9.0531	8.4145	8.5504	8.4099
0.05	9.6853	9.2310	8.5724	8.7099	8.5677
0.075	9.8492	9.3978	8.7210	8.8597	8.7160
0.1	10.0034	9.5550	8.8613	9.0011	8.8562
0.25	10.7720	10.3403	9.5712	9.7140	9.5653
0.5	11.6667	11.2572	10.4282	10.5687	10.4212
0.75	12.2830	11.8896	11.0459	11.1807	11.0381
1.0	12.7348	12.3533	11.5172	11.6454	11.5088
1.25	13.0805	12.7081	11.8907	12.0122	11.8819
1.5	13.3536	12.9885	12.1950	12.3099	12.1858
1.75	13.5749	13.2156	12.4481	12.5571	12.4386
2.0	13.7579	13.4035	12.6623	12.7657	12.6526
3.0	14.2546	13.9132	13.2690	13.3548	13.2590
4.0	14.5482	14.2144	13.6479	13.7212	13.6379
5.0	14.7421	14.4133	13.9077	13.9721	13.8979
6.0	14.8798	14.5545	14.0972	14.1550	14.0878
8.0	15.0622	14.7416	14.3556	14.4042	14.3468
10.0	15.1777	14.8600	14.5236	14.5664	14.5155
50.0	15.5813	15.2737	15.1427	15.1668	15.1398
100.0	15.6357	15.3295	15.2306	15.2530	15.2289
∞	15.6912	15.3864	15.3211	15.3424	15.3211

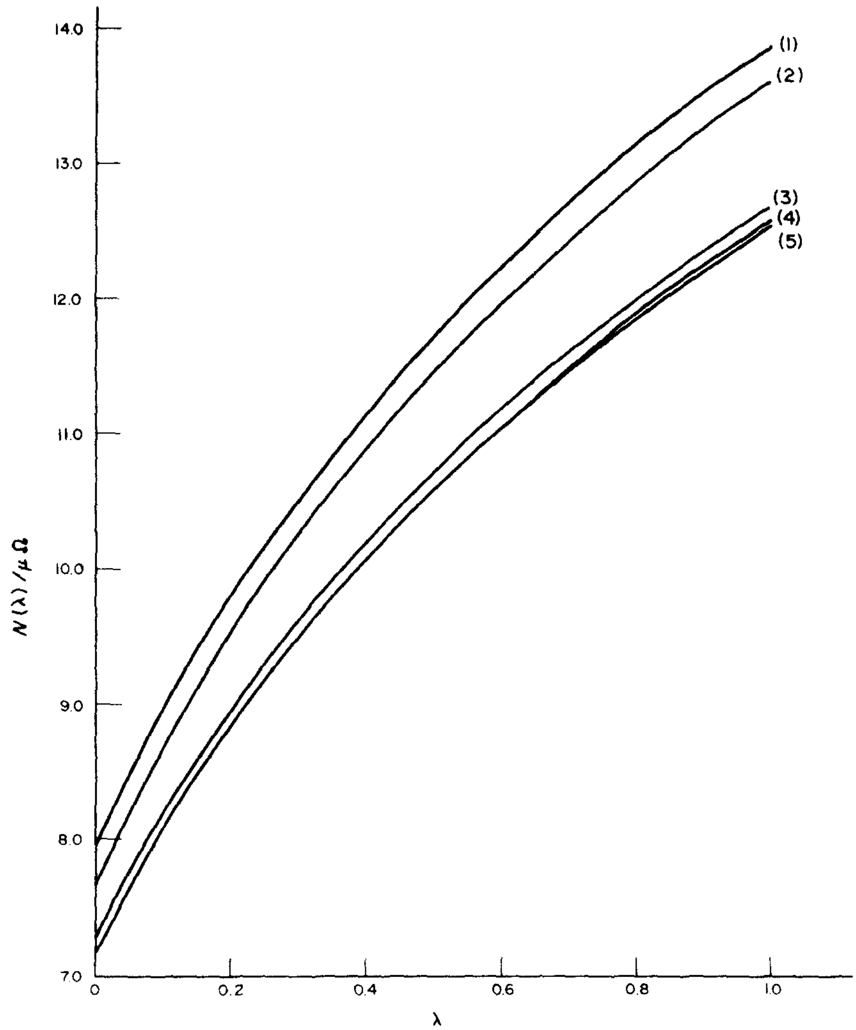

Figure 1. Graph of $N(\lambda)/\mu\Omega$ vs λ for $0 \leq \lambda \leq 1$, $h = 0.125$ and (1) $H = 1.0$, $b = 2.0$; (2) $H = 2.0$, $b = 2.0$; (3) $H = 2.0$, $b = 100.0$; (4) $H = 10.0$, $b = 10.0$; (5) $H = 100.0$, $b = 100.0$.

$N(\lambda)/N(0)$, where $N(0)$ is the couple when the surface is free of contaminant. Tables 3 and 4 show this ratio for $h = 0.125$ and $h = 0.25$ respectively.

We turn next to the surface velocity profiles, again for $H = 1$ and $b = 2$. These are sketched in figures 3 and 4 for $h = 0.125$ and $h = 0.25$ respectively, and various values of λ.

The maximum surface velocity $v_{\max}$ is of practical value (see the discussion in I) and tables 5 and 6 give $\Omega^{-1}v_{\max}$ and ΩT, where T is the periodic time of revolution of a surface particle, calculated at the values of ρ shown in the final column of the tables, at which $\Omega^{-1}v(\rho, -h)$ is a maximum. Comparison with infinite fluid values of $v_{\max}$ and ΩT shows that the boundary effects are much less than in the case of the couple, e.g. when $\lambda = 0.1$ the presence of the finite boundary changes the periodic time by less than 2 per cent.

6. CONCLUDING REMARKS

In this paper we have given a comprehensive treatment, both asymptotic and numerical, of finite container boundary effects for the rotational surface viscometer proposed in I. An accurate calculation of such boundary effects is clearly necessary since their presence can easily mask variations in, for example, the resistive couple on the rotating body due to the surfactant film. Oh & Slattery (1978) have considered finite container problems for an interface viscometer, but the mathematical techniques employed are very different from those used here.

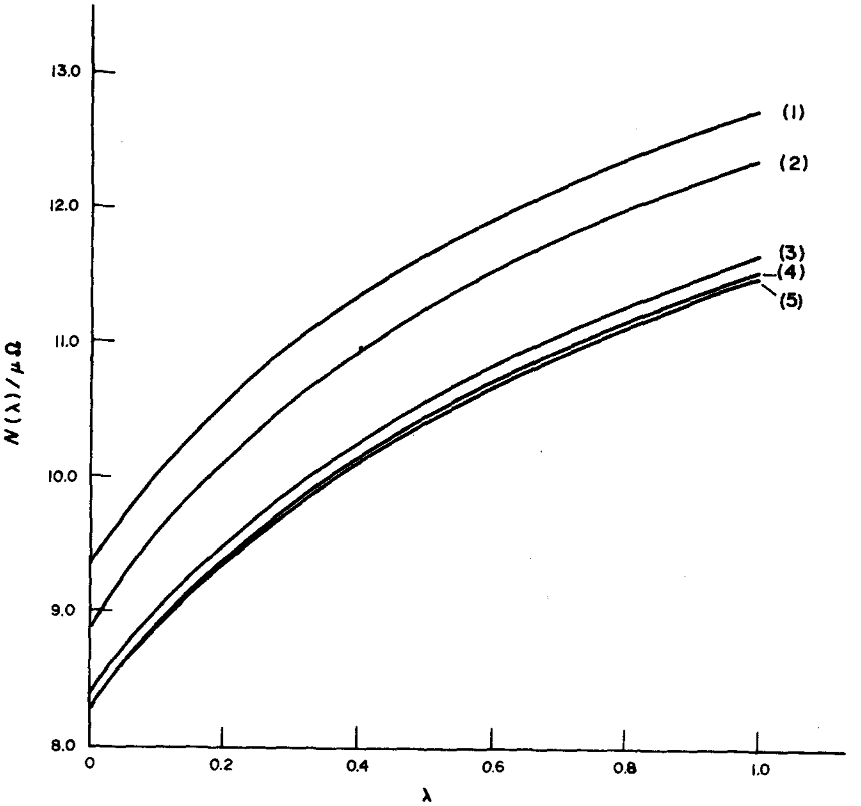

Figure 2. Graph of $N(\lambda)/\mu\Omega$ vs λ for $0 \le \lambda \le 1$, $h = 0.25$ and (1) $H = 1.0$, $b = 2.0$; (2) $H = 2.0$, $b = 2.0$; (3) $H = 2.0$, $b = 100.0$; (4) $H = 10.0$, $b = 10.0$; (5) $H = 100.0$, $b = 100.0$.

Table 3. Values of $N(\lambda)/N(0)$ for $h = 0.125$ and various values of λ, H and b

λ	H = 1.0 b = 2.0	H = 2.0 b = 2.0	H = 10.0 b = 10.0	H = 2.0 b = 100.0	H = 100.0 b = 100.0
0	1.0000	1.0000	1.0000	1.0000	1.0000
0.025	1.0355	1.0367	1.0346	1.0347	1.0346
0.05	1.0686	1.0710	1.0669	1.0670	1.0669
0.075	1.0998	1.1034	1.0974	1.0975	1.0974
0.1	1.1294	1.1342	1.1264	1.1265	1.1264
0.25	1.2831	1.2945	1.2773	1.2770	1.2772
0.5	1.4793	1.4999	1.4729	1.4711	1.4726
0.75	1.6287	1.6564	1.6252	1.6217	1.6247
1.0	1.7469	1.7803	1.7487	1.7434	1.7482
1.25	1.8430	1.8811	1.8516	1.8444	1.8509
1.50	1.9228	1.9648	1.9388	1.9298	1.9380
1.75	1.9902	2.0353	2.0138	2.0032	2.0129
2.0	2.0477	2.0957	2.0791	2.0670	2.0782
3.0	2.2135	2.2694	2.2738	2.2565	2.2727
4.0	2.3185	2.3795	2.4030	2.3820	2.4019
5.0	2.3911	2.4556	2.4954	2.4715	2.4943
6.0	2.4443	2.5113	2.5647	2.5387	2.5636
8.0	2.5169	2.5873	2.6620	2.6328	2.6611
10.0	2.5642	2.6369	2.7271	2.6958	2.7263
50.0	2.7384	2.8192	2.9796	2.9413	2.9802
100.0	2.7630	2.8450	3.0172	2.9781	3.0181
∞	2.7883	2.8715	3.0563-	3.0167	3.0577

Table 4. Values of $N(\lambda)/N(0)$ for $h = 0.25$ and various values of λ, H and b

λ	H = 1.0 b = 2.0	H = 2.0 b = 2.0	H = 10.0 b = 10.0	H = 2.0 b = 100.0	H = 100.0 b = 100.0
0	1.0000	1.0000	1.0000	1.0000	1.0000
0.025	1.0202	1.0215	1.0205	1.0204	1.0205
0.05	1.0389	1.0416	1.0396	1.0394	1.0396
0.075	1.0565	1.0604	1.0576	1.0573	1.0576
0.1	1.0731	1.0781	1.0747	1.0742	1.0746
0.25	1.1555	1.1667	1.1608	1.1592	1.1607
0.5	1.2515	1.2702	1.2647	1.2612	1.2645
0.75	1.3176	1.3415	1.3396	1.3343	1.3394
1.0	1.3661	1.3939	1.3968	1.3897	1.3965
1.25	1.4031	1.4339	1.4420	1.4335	1.4418
1.5	1.4324	1.4655	1.4789	1.4690	1.4786
1.75	1.4562	1.4912	1.5096	1.4985	1.5093
2.0	1.4758	1.5124	1.5356	1.5234	1.5353
3.0	1.5291	1.5699	1.6092	1.5937	1.6089
4.0	1.5606	1.6039	1.6551	1.6374	1.6548
5.0	1.5814	1.6263	1.6867	1.6674	1.6864
6.0	1.5961	1.6422	1.7096	1.6892	1.7094
8.0	1.6157	1.6633	1.7410	1.7189	1.7408
10.0	1.6281	1.6767	1.7614	1.7383	1.7613
50.0	1.6714	1.7234	1.8364	1.8100	1.8371
100.0	1.6772	1.7297	1.8471	1.8202	1.8479
∞	1.6832	1.7361	1.8581	1.8309	1.8591

Table 5. Values of $\Omega^{-1}v(\rho, -h)$ and ΩT calculated at the points where $\Omega^{-1}v(\rho, -h)$ is a maximum, with $h = 0.125$, $H = 1.0$, $b = 2.0$ and a range of values of λ

λ	$\Omega^{-1}v_{max}$	ΩT	ρ
0	0.8176	6.9163	0.9
0.025	0.7906	7.0734	0.89
0.05	0.7681	7.2801	0.89
0.075	0.7486	7.3865	0.88
0.1	0.7308	7.4796	0.87
0.25	0.6496	8.3186	0.86
0.5	0.5569	9.5904	0.85
0.75	0.4901	10.7684	0.84
1.0	0.4385	11.8937	0.83
1.25	0.3970	13.1850	0.83
1.50	0.3629	14.1999	0.83
1.75	0.3342	15.6030	0.83
2.0	0.3098	16.6298	0.82
3.0	0.2399	21.4734	0.82
4.0	0.1958	26.3080	0.82
5.0	0.1655	31.1387	0.82

We have concentrated our numerical efforts on the case of the rotating disk but a similar treatment of the rotating sphere can be given. It does not seem to be possible to use the bispherical coordinate formulation of Davis & O'Neill (1979) for the finite container geometry, but an integral equation of the second kind, analogous to [37] and amenable to numerical solution, can be derived. However, since the surfactant effects in the rotating sphere case are less pronounced than for the disk, we have not thought it worthwhile to pursue this analysis.

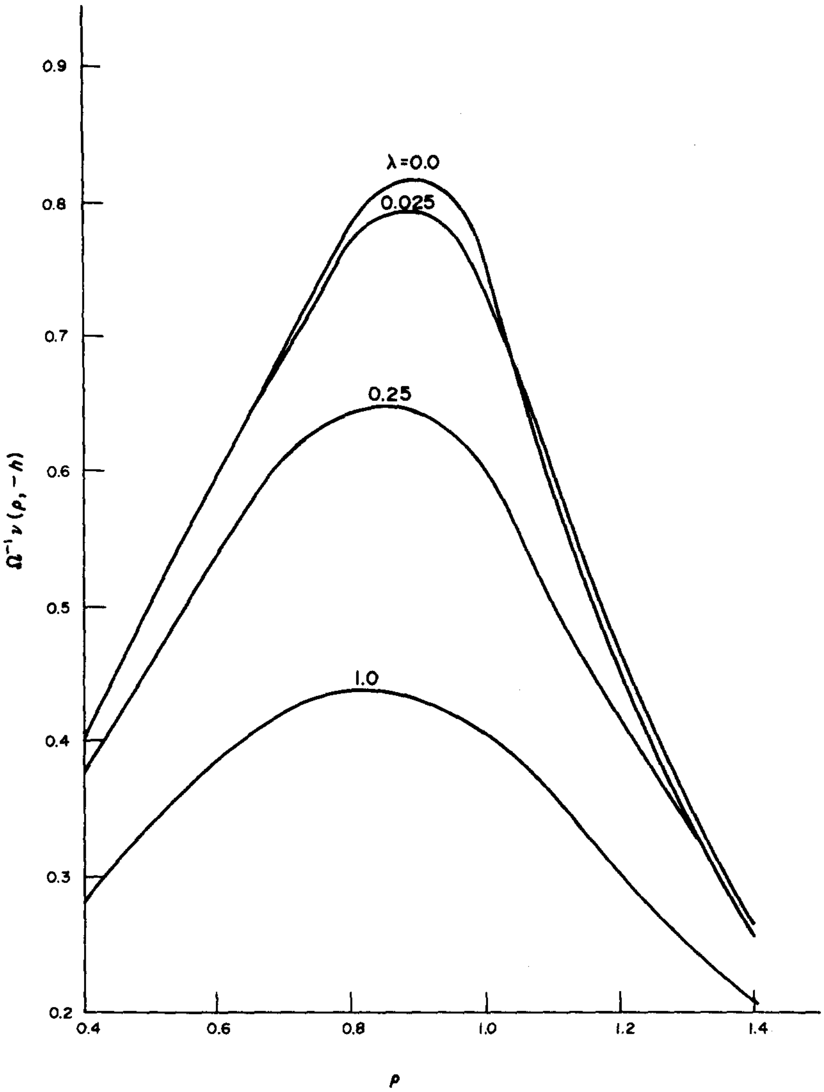

Figure 3. Velocity profiles for $\lambda = 0.0, 0.025, 0.25$ and 1.0 with $h = 0.125$, $H = 1.0$, $b = 2.0$.

Table 6. Values of $\Omega^{-1}v(\rho, -h)$ and ΩT calculated at the points where $\Omega^{-1}v(\rho, -h)$ is a maximum, with $h = 0.25$, $H = 1.0$, $b = 2.0$ and a range of values of λ

λ	$\Omega^{-1}v_{max}$	ΩT	ρ
0	0.6727	7.9393	0.85
0.025	0.6474	8.2494	0.85
0.05	0.6250	8.5457	0.85
0.075	0.6048	8.7272	0.84
0.1	0.5863	9.0020	0.84
0.25	0.4992	10.4460	0.83
0.5	0.4039	12.9126	0.83
0.75	0.3401	15.3321	0.83
1.0	0.2941	17.7330	0.83
1.25	0.2591	20.1247	0.83
1.50	0.2317	22.5112	0.83
1.75	0.2095	24.8944	0.83
2.0	0.1912	27.2754	0.83
3.0	0.1418	36.7876	0.83
4.0	0.1127	46.2909	0.83
5.0	0.0935	55.7905	0.83

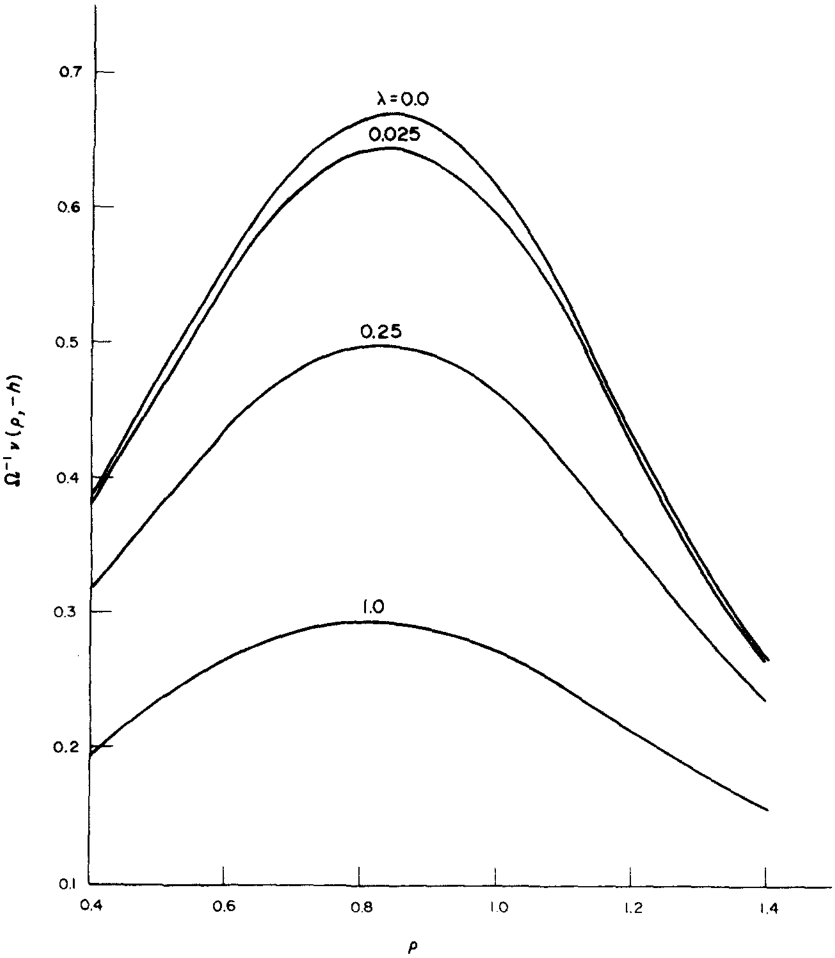

Figure 4. Velocity profiles for $\lambda = 0.0, 0.025, 0.25$ and 1.0 with $h = 0.25$, $H = 1.0$, $b = 2.0$.

REFERENCES

Brenner, H. 1962 Effect of finite boundaries on the Stokes resistance of an arbitrary particle. *J. Fluid Mech.* **12**, 35–48.

Clenshaw, C. W. & Curtis, A. R. 1960 A method for numerical integration on an automatic computer. *Numer. Math.* **2**, 197–205.

Davis, A. M. J. & O'Neill, M. E. 1979 The slow rotation of a sphere submerged in a fluid with a surfactant surface layer. *Int. J. Multiphase Flow* **5**, 413–425.

El-Gendi, S. E. 1969 Chebyshev solution of differential, integral and integro-differential equations. *Computer J.* **12**, 282–287.

Oh, S. G. & Slattery, J. C. 1978 Disk and biconical interfacial viscometers. *J. Colloid Int. Sci.* **67**, 516–525.

Rayleigh, J. W. S. 1965 *The Theory of Sound*, Vol. 1, pp. 200–202. Dover, New York.

Shail, R. 1979 The slow rotation of an axisymmetric solid submerged in a fluid with a surfactant surface layer—I. The rotating disk in a semi-infinite fluid. *Int. J. Multiphase Flow* **5**, 169–183.

APPENDIX

In this appendix we give a derivation of the Green's function G, used in the body of the paper. The function $G(\rho, z, \phi; \rho', z', \phi)$ satisfies the equation

$$\nabla^2 G = -\frac{4\pi}{\rho}\delta(\rho-\rho')\delta(\phi-\phi')\delta(z-z'), \qquad [A1]$$

and the boundary conditions

$$G = 0 \text{ on } \rho = b, -h \le z \le H - h, \quad \text{[A2]}$$

$$G = 0 \text{ on } z = H - h, 0 \le \rho \le b, \quad \text{[A3]}$$

and

$$\frac{\partial G}{\partial z} - \lambda \frac{\partial^2 G}{\partial z^2} = 0 \text{ on } z = -h, 0 \le \rho \le b. \quad \text{[A4]}$$

Using the method of separation of variables, a solution of [A1] which satisfies [A2]–[A4] is given by

$$G = \sum_{r=0}^{\infty} \sum_{n=1}^{\infty} D_{r,n} \left\{ K_r(p_n\rho >) I_r(p_n\rho <) - I_r(p_n\rho) I_r(p_n\rho') \frac{K_r(p_nb)}{I_n(p_nb)} \right\}$$

$$\times \sin p_n(z - H + h) \sin p_n(z' - H + h) \cos r(\phi - \phi'), \quad \text{[A5]}$$

where p_n, $n = 1, 2, \ldots$, are the positive roots in ascending order of magnitude of the equation

$$\cos pH - \lambda p \sin pH = 0, \quad \text{[A6]}$$

and $\rho > = \max(\rho, \rho')$, $\rho < = \min(\rho, \rho')$. In [A5] the $D_{r,n}$ are constants determined by substitution of [A5] in [A1]. This substitution yields the relation

$$\sum_{n=1}^{\infty} D_{s,n} \sin p_n(z - H + h) \sin p_n(z' - H + h) = 2(2 - \delta_{s0})\delta(z - z'), -h \le z, z' \le H - h. \quad \text{[A7]}$$

However the set of functions $\sin p_n(z - H + h)$, $n = 1, 2, 3, \ldots$, whilst complete, is not an orthogonal set on $-h < z < H - h$, and hence a method due to Rayleigh (1894) must be used to expand $\delta(z - z')$ in terms of the set. This result is

$$\delta(z - z') = \sum_{n=1}^{\infty} \frac{4p_n \sin p_n(z - H + h) \sin p_n(z' - H + h)}{2p_nH + \sin 2p_nH}, \quad \text{[A8]}$$

whence

$$D_{s,n} = \frac{8p_n(2 - \delta_{s0})}{2p_nH + \sin 2p_nH}, \quad \text{[A9]}$$

giving the required Green's function in the form

$$G = \sum_{r=0}^{\infty} \sum_{n=1}^{\infty} \frac{8p_n(2 - \delta_{s0}) \cos r(\phi - \phi')}{2p_nH + \sin 2p_nH} \left\{ K_r(p_n\rho >) I_r(p_n\rho <) \right.$$

$$\left. - I_r(p_n\rho) I_r(p_n\rho') \frac{K_r(p_nb)}{I_r(p_nb)} \right\} \sin p_n(z - H + h) \sin p_n(z' - H + h). \quad \text{[A10]}$$

It follows from [A1] that G can be written as

$$G = \frac{1}{R} + G_1, \quad \text{[A11]}$$

where R is the distance between the points (ρ, ϕ, z) and (ρ', ϕ', z') and G_1 is regular when $\rho = \rho'$, $\phi = \phi'$, $z = z'$. Equation [A10] is not in the form [A11], but can be easily converted so as to display the inverse distance contribution. We note that G^*, where

$$G^* = \lim_{b\to\infty} G = \sum_{r=0}^{\infty}\sum_{n=1}^{\infty} \frac{8p_n(2-\delta_{r0})\cos r(\phi-\phi')}{2p_nH + \sin 2p_nH} K_r(p_n\rho<)I_r(p_n\rho<)$$
$$\times \sin p_n(z-H+h)\sin p_n(z'-H+h)\,, \qquad \text{[A12]}$$

is the Green's function for an infinite stratum of fluid of depth H with a surfactant layer. An alternative form for G^* is given by the method of separation of variables as

$$G^* = \sum_{r=0}^{\infty}(2-\delta_{r0})\cos r(\phi-\phi')\int_0^\infty J_r(\xi\rho)J_r(\xi\rho')\mathrm{e}^{-\xi(z-z')}\mathrm{d}\xi$$
$$+\sum_{r=0}^{\infty}(2-\delta_{r0})\cos r(\phi-\phi')\int_0^\infty [(1-\lambda\xi)\{\mathrm{e}^{-\xi(2h-H)}\cosh\xi(z+z') - \mathrm{e}^{-\xi H}\cosh\xi(z-z')\}$$
$$-\mathrm{e}^{-\xi(z+z')}\{\cosh\xi(2h-H) + \lambda\xi\sinh\xi(2h-H)\}]\frac{J_r(\xi\rho)J_r(\xi\rho')}{\cosh\xi H + \lambda\xi\sinh\xi H}\mathrm{d}\xi. \qquad \text{[A13]}$$

The first term in [A13] is the expansion of the singular inverse distance Green's function in cylindrical polar coordinates. The required modification of [A10] now follows by replacing that part of [A10] expressed in [A12] by [A13], and the coefficient of $\cos(\phi-\phi')$ is seen to be identical with [7].